WARWICK
THE UNIVERSITY OF WARWICK

Manuscript version: Author's Accepted Manuscript
The version presented in WRAP is the author's accepted manuscript and may differ from the published version or Version of Record.

Persistent WRAP URL:
http://wrap.warwick.ac.uk/150274

How to cite:
Please refer to published version for the most recent bibliographic citation information. If a published version is known of, the repository item page linked to above, will contain details on accessing it.

Copyright and reuse:
The Warwick Research Archive Portal (WRAP) makes this work by researchers of the University of Warwick available open access under the following conditions.

Copyright © and all moral rights to the version of the paper presented here belong to the individual author(s) and/or other copyright owners. To the extent reasonable and practicable the material made available in WRAP has been checked for eligibility before being made available.

Copies of full items can be used for personal research or study, educational, or not-for-profit purposes without prior permission or charge. Provided that the authors, title and full bibliographic details are credited, a hyperlink and/or URL is given for the original metadata page and the content is not changed in any way.

Publisher's statement:
Please refer to the repository item page, publisher's statement section, for further information.

For more information, please contact the WRAP Team at: wrap@warwick.ac.uk.

warwick.ac.uk/lib-publications

The role of nuclear quantum effects in the relative stability of hexagonal and cubic ice

Samuel J. Buxton,[1] David Quigley,[2] and Scott Habershon[1, a)]

[1)] *Department of Chemistry and Centre for Scientific Computing, University of Warwick, Coventry, CV4 7AL, United Kingdom*

[2)] *Department of Physics and Centre for Scientific Computing, University of Warwick, Coventry, CV4 7AL, United Kingdom*

At atmospheric pressure, hexagonal ice (I_h) is thermodynamically stable relative to cubic ice (I_c), although the magnitude and underlying physical origin of this stability difference are not well defined. Pure I_c crystals are not accessible experimentally, and hence computer simulations have often been used to interrogate the relative stabilities of I_h and I_c; however, these simulations are dominated by molecular interaction models which ignore the intramolecular flexibility of individual water molecules, do not describe intermolecular hydrogen-bonding with sufficient accuracy, or ignore the role of nuclear quantum effects (NQEs) such as zero-point energy. Here, we show that when comparing the relative stability of I_h and I_c using a flexible, anharmonic molecular interaction model, while also accurately accounting for NQEs, a new picture emerges: I_h is stabilised relative to I_c as a result of subtle differences in the intramolecular geometries and intermolecular interactions of water molecules which are modulated by NQEs. Our simulations hence suggest that NQEs are a major contributor to the stabilisation of I_h under terrestrial conditions, and thus contribute to the well-known hexagonal (six-fold) symmetry of ice crystals.

[a)] Electronic mail: S.Habershon@warwick.ac.uk

I. INTRODUCTION

The thermodynamics and kinetics associated with the nucleation and crystallization of ice remains a challenge to both experimental and computational chemistry. Under terrestrial conditions, hexagonal ice I_h is the thermodynamically-stable form, leading to the well-known six-fold symmetry commonly observed in snowflakes. However, both experimental investigations and computer simulations have indicated that I_h is *only just* the thermodynamically-preferred ice polymorph. In particular, it is predicted that the cubic ice polymorph (I_c) is only $\sim$30-150 $\mathrm{J\,mol^{-1}}$ higher in free energy than I_h at typical temperatures accessible on Earth,[1–3] an extremely small energy difference which tips the balance of stability in favour of I_h, such that pure I_c crystals have never been observed to date.

Resolving the small free energy difference between the I_h and I_c polytypes of ice I stands as a challenge to our current understanding of hydrogen-bonding in water and ice. The structure of I_h comprises alternating double-layers of water molecules stacked in an $ABAB\ldots$ arrangement. The hydrogen-bonding structure of I_h is determined by the Bernal-Fowler 'ice rules';[4] there is no proton ordering, but each oxygen atom participates in two short (covalent) O-H hydrogen bonds, and two long (intermolecular) hydrogen bonds. The I_c polymorph also obeys the 'ice rules', but the stacking arrangement of hydrogen-bonded layers in I_c follows the $ABCABC\ldots$ pattern of cubic close-packed systems. In addition, so-called stacking-disordered ices,[5] in which stacking patterns intermediate between those of I_h and I_c, are also observed; stacking-disordered ice variants are strongly implicated in the nucleation process of ice, particularly in the lower-temperature conditions found in the upper atmosphere[6–8].

Based on their known (or predicted) physical properties, I_h and I_c are found to behave in surprisingly similar fashions, despite their different stacking patterns. The calculated vibrational spectra of these two different ice forms are very similar,[9–11] highlighting the similar local hydrogen-bonding environments created by the proton disorder. In addition, the density, thermal expansivity and configurational entropy of I_h and I_c are all found to be very similar.[12–14] The main structural differences between I_h and I_c become evident in simulated radial distribution functions (RDFs), where it is found that the first-nearest-neighbour environment in each structure is essentially identical, but with the oxygen sub-lattices of I_h and I_c showing pronounced differences in the second neighbour shell and beyond;[9,10] these differences are a consequence of the different oxygen hexamer arrangements in the two structures,

with I_h exhibiting both chair- and boat-type hexamers, whereas I_c exhibits only chair-type hexamers.

Because I_c cannot (to date) be prepared in a pure crystalline form (and noting that much experimental data on notionally cubic ice actually corresponds to the stacking-disordered form with varying degrees of cubicity), computer simulations have been one of the most commonly applied tools to investigate the relative thermodynamic stability of pure I_h and pure I_c. Several previous studies have employed empirical water models in which the water monomer geometries are fixed at some idealized reference geometry (*e.g.* the TIP4P family of water models[10,12,14–16]); combined with normal mode analysis and standard expressions for (classical or quantum) partition functions, these simulations have suggested that the differing vibrational density-of-states in the librational region give rise to the lower free energy of I_h. Going beyond empirical models, several studies have employed density functional theory (DFT) to calculate the ice vibrational density-of-states and corresponding quantum partition functions and free energies.[9,17,18] Most relevant for this work, DFT simulations (with the PBE functional) have been used to calculate both harmonic and anharmonic free energies for I_c and I_h; contrary to the previous TIP4P-based simulations, these DFT results suggest that anharmonicity, particularly in the O-H stretching region of the spectrum, is responsible for the relative free energy ordering of I_h and I_c.[9]

However, none of these previous simulations have been able to provide a complete picture or explanation of the relative stability of ice I_h and I_c. For example, simulations based on the single-site mW model posses no librational motion nor O-H bonds and hence the two polytypes might be expected to posses equal stability. The stability of I_h relative to I_c has been accurately quantified for this model[7] and is indeed very much smaller than the enthalpy released per mole when stacking disordered ice transforms to ice $I_h$in calorimetry experiments. Nevertheless, the mW model is apparently consistent with calculations of the relative I_h / I_c stability extracted from fitting a model of dislocation loop shrinkage dynamics to experiment[19,20], suggesting either a problem with the defect dynamics model, or with the calorimetry experiments. Other popular models based on TIP4P and similar rigid water geometries also neglect the role of intramolecular flexibility;[10,12,14–16] previous simulations have shown that the competition between intramolecular molecular geometry distortion and intermolecular interactions can have an important bearing on predicted physical properties in water and other hydrogen-bond systems.[21] In addition, calculated free energies based on

harmonic analysis (or its vibrational self-consistent field (VSCF) extension to include anharmonicity) do not sample the fully-coupled configurational fluctuations associated with thermal motion; this is most obvious in calculated vibrational spectra in the O-H region, which tend to exhibit more well-defined peaks in harmonic (and self-consistent) analyses, rather than the broadened vibrational peaks observed in experiment or direct molecular dynamics (MD) simulations. Furthermore, it is also worth noting that previous DFT simulations using VSCF predict an anharmonic free energy difference of around 630 J/mol, which is difficult to reconcile against experimental measurements of the enthalpy released upon transformation of stacking disordered ice into I_h.[9] Finally, nuclear quantum effects (NQEs[22–27]) such as zero-point energy are most commonly treated by using either quantum harmonic-oscillator partition functions,[10,14] or by explicit calculation of vibrational eigenstates in a self-consistent field picture;[9,17,18] the explicitly-correlated effects of NQEs on sampled configurational space and unit cell fluctuations are therefore usually ignored. As we show here, once one accounts fully for the influence of NQE, configurational sampling and anharmonicity, a different picture of the relative stability of I_h and I_c emerges.

The main aims of this paper are three-fold. First, we investigate what the empirical q-TIP4P/F water model predicts with regards to the influence of NQEs on the relative stability of I_h and I_c using direct free energy calculations for the different ice phases. Second, we investigate the impact of anharmonicity in the relative stability of I_h and I_c. Finally, we attempt to rationalize the role of NQEs on the I_h and I_c stability on simple geometric and energetic grounds. As we show here, once one accounts fully for the influence of NQE, configurational sampling and anharmonicity, a more complete picture of the relative stability of I_h and I_c emerges.

II. SIMULATION DETAILS

We have performed a series of molecular simulations to assess the free energy difference between I_h and I_c while simultaneously accounting for the role of NQE, configurational sampling and vibrational anharmonicity.[23,28] Our simulations employed the empirical q-TIP4P/F model to describe intra- and intermolecular interactions.[21] This model describes the intramolecular O-H stretching motions using an anharmonic quartic expansion of a Morse potential, while the potential energy contribution due to intramolecular H-O-H bend-

ing is described using a harmonic function of the bend angle. Intermolecular interactions are described using Lennard-Jones dispersion terms between oxygen atoms on different water molecules, along with Coulomb interactions between fixed partial-charges positioned on each hydrogen atom and at an off-atom site along the H-O-H bisector. The q-TIP4P/F model was parameterised such that several experimental observables, particularly RDFs, diffusion coefficients and infrared vibrational frequencies, were reproduced for liquid water when performing quantum-mechanical (path-integral-based) simulations; further simulations with q-TIP4P/F have shown that it gives a good approximation of a number of other properties which were not included in the original parameterisation, including the melting temperature of I_h and the well-known liquid density anomaly.[21] Of particular relevance in this work is the fact that q-TIP4P/F exhibits "competition" between intramolecular and intermolecular NQEs; this feature has been shown to be responsible for the ability of q-TIP4P/F to correctly account for NQEs in diffusion coefficients, isotopic fractionation ratios,[29] solvent exchange around ion solvation shells,[30] and proton momentum distributions.[31] Of course, we acknowledge that q-TIP4P/F is an approximate interaction model and does not capture all aspects of NQEs in liquid water; for example, it is well known that the anomalous trend in molar volumes of H_2O and D_2O is not captured by q-TIP4P/F.[32] However, as noted further below, recent alternative simulations[33] performed using a machine-learned PES based on revPBE0 reproduce the effects we discuss here (although do not provide the same structural interpretation as is enabled by our results). This finding, as well as the detailed characterization of q-TIP4P/F which is now available, give us some degree of confidence that the role of NQEs in the relative free energies of I_c and I_h are correctly captured here.

We have calculated the Gibbs free energy of I_h and I_c using the q-TIP4P/F water model at a pressure of 1 bar and temperatures ranging from 200 K to 250 K; the (classical) melting point of I_h using the q-TIP4P/F water model is 258 K,[21,23,28] so our temperature range of interest spans a regime in which I_h is naturally expected to be thermodynamically stable in the bulk limit. Our molecular dynamics simulations for both I_h and I_c were performed with simulation cells containing 432 water molecules in periodic boundary conditions; initial oxygen atom positions were chosen according to the known ice structures, while the hydrogen atoms were positioned according to the Bernal-Fowler ice-rules[4] using a Monte Carlo algorithm to sample different proton orderings[34], leading to fully-disordered proton arrangements. Notably, this approach, and the simulation box sizes, gives access to proton

configurations which can't be obtained by repeating a single unit cell. All calculated free energies (both classical and quantum-mechanical) were averaged over three different proton-disordered simulation cells for both I_h and I_c. Following previous work,[28] *classical* (that is, completely neglecting the role of NQEs) free energies of I_c and I_h were calculated in a two-step process: (i) The Debye crystal free energy for molecular models of each ice structure were evaluated in averaged unit cells obtained in classical isothermal-isobaric MD simulations of the respective ice structure, and (ii) The free energy difference between the Debye crystal and the fully-interacting q-TIP4P/F model was evaluated using Thermodynamic integration (TI) simulation along an order parameter which connects these two different descriptions of the ice structure. Together, these two free energy contributions (Debye crystal free energy and thermodynamic integration to q-TIP4P/F model) yielded the final classical free energies of I_h and I_c. To calculate *quantum-mechanical* free energies (that is, completely accounting for the role of NQEs), we used the well-known path-integral molecular dynamics (PIMD) methodology. In particular, we perform TI using isothermal-isobaric PIMD simulations along an order parameter which connects the fully-classical description of the ice structure to a fully-quantum PIMD system;[23] the free energy difference along this path is added to the known classical free energy to obtain the quantum free energy. It is important to emphasise that our classical and quantum simulations give the exact free energy of the ice structures for the q-TIP4P/F water model (within statistical errors); all relevant effects, notably configurational sampling (of both individual water molecules and unit cell fluctuations), anharmonicity and NQEs, are correctly included in our simulations. Further details, such as details of the q-TIP4P/F model and simulation times, can be found in *Supplementary Information*.

III. RESULTS AND DISCUSSION

Figure 1(a) shows the calculated free energy difference between I_h and I_c for the q-TIP4P/F water model at temperatures between 200 K and 250 K, as determined in both classical and quantum simulations. In the case of the classical free energy difference, we find that I_h is more stable than I_c by about 10 J/mol across the whole temperature range; in other words, q-TIP4P/F finds that I_h is more stable than I_c, although the free energy difference is smaller than the expected $\sim$30 -150 J/mol range.[1–3,9]

However, a key conclusion of this work is that the quantum-mechanical free energy difference between I_h and I_c is much greater than the classical result; for the anharmonic q-TIP4P/F water model, we find that NQEs stabilise I_h relative to I_c by up to 30 J/mol. This is a significant contribution which brings the calculated free energy difference from a few J/mol (similar to the mW model) into much better agreement with the order-of-magnitude expected based on experimental estimates. However, the most interesting observation is that, while classical simulations show that I_h is only just thermodynamically-stable relative to I_c, our simulations show, for the first time, that NQE are a significant driver in determining the relative stabilities of these ice polytypes. As an aside, we note that the (classical and quantum) free energy differences between different proton configurations is of the order of 5-10 J/mol for both $I_c$and I_h; the stabilizing effect of NQEs is more significant than the differences due to different proton configurations.

Why do NQEs result in stabilisation of I_h relative to I_c? In answering this question, we first consider the role of anharmonicity in the relative free energies of I_h and I_c; in particular, previous path-integral-based simulations of aqueous systems have shown that harmonic and anharmonic interaction models can give rise to largely different behaviours in predicted physical properties, particularly when NQEs are important.[21,29,35,36] Furthermore, recent simulations have suggested that vibrational anharmonicity, particularly in the higher-frequency O-H vibrational modes, serves to stabilise I_h over I_c;[9] these simulations employed DFT, along with either harmonic analysis or VSCF, in order to calculate the vibrational spectra, vibrational partition function and free energies of I_h and I_c. Investigating the role of O-H vibrational anharmonicity in our direct free energy calculations is straightforward; because the intramolecular potential energy term in q-TIP4P/F employs all terms up to fourth-order in the O-H bond distance, we can derive a corresponding harmonic model by simply truncating this expansion at the quadratic term (See *Supplementary Information*). Repeating our classical and quantum free energy calculations using this harmonic version of q-TIP4P/F (with all other terms in the model as in the original q-TIP4P/F potential) gives the results in Fig. 1(b); we find that the relative free energies of I_h and I_c are essentially unchanged relative to the fully anharmonic q-TIP4P/F model, suggesting no significant role for O-H anharmonicity in our simulations.

A possible origin for the difference between our results and previous work with regards to the role of anharmonicity is the different interaction models employed; we used an em-

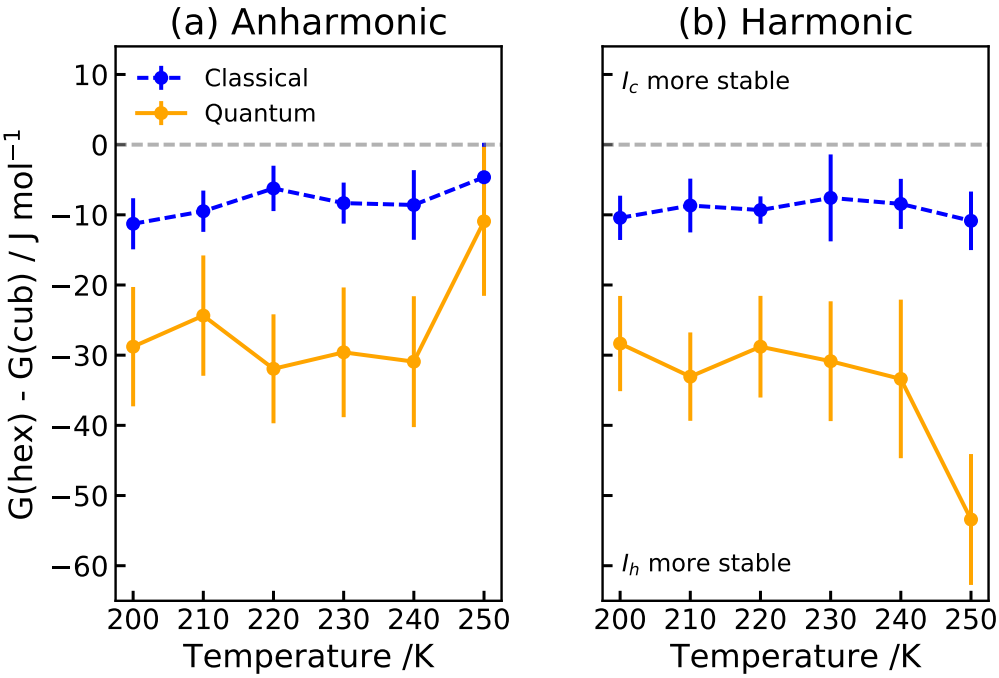

FIG. 1: (a) Free energy difference between I_h and I_c calculated in classical (blue dashed line) and quantum-mechanical (orange solid line) simulations of the anharmonic q-TIP4P/F water model. (b) Free energy difference between I_h and I_c calculated in classical (blue dashed line) and quantum-mechanical (orange solid line) simulations of a harmonic version of the q-TIP4P/F water model, with the intramolecular O-H stretching term truncated at quadratic level. In both (a) and (b), negative free energy differences correspond to I_h being more thermodynamically stable than I_c. The error bars represent one standard error in the free energy values calculated for the three different proton-disordered configurations used in each calculation (see *Supplementary Information*).

pirical force-field, whereas Engel *et al* employed DFT with the PBE exchange-correlation functional.[9] However, it is well known that PBE consistently "overbinds" molecules in hydrogen-bonded systems;[37] for example, liquid water RDFs calculated using PBE are strongly over-structured, the liquid water diffusion coefficient calculated with PBE is typically predicted to be too small (usually by a factor of ∼2-4[37,38]) relative to experiment, and the I_h melting point is estimated to be ∼420 K when calculated using the PBE functional,[39] an over-estimate of around 150 K compared to experiment. In contrast, q-TIP4P/F is now well-established as providing a surprisingly accurate description of liquid water; the liquid density (and its temperature-dependence) behaves correctly, the liquid diffusion coefficients and RDFs are in excellent agreement with experiment, and the I_h melting point (calculated using quantum free energy calculations) for q-TIP4P/F is 251 K (just 22 K lower

than experiment). In regards to calculating vibrational contributions to free energy values, the PBE functional is known to give a poor reproduction of vibrational frequencies in hydrogen-bonded clusters, specifically $(H_2O)_n$ (n=2-6); comparison of harmonic frequencies determined with PBE to CCSD(T) benchmarks shows that PBE vibrational frequencies can be in error by an average of 100 cm^{-1} (and even up to 500 cm^{-1}).[40] The q-TIP4P/F model has been found to demonstrate errors of up to 100 cm^{-1} for some vibrational bands for H_2O_6[41], although the vibrational spectrum of liquid water is specifically tuned to give good agreement with experiment in q-TIP4P/F[21] and the anharmonic vibrational component of this model has been found to be essential in reproducing isotopic fractionation ratios.[29] Finally, it is also important to note that the simulations on the q-TIP4P/F potential performed here yield the exact classical and quantum-mechanical free energy values (within statistical error), fully accounting for explicit correlation between all water molecules, as well as explicit correlation between the molecular configuration and the unit cell; in the case of VSCF-type calculations, used in combination with DFT calculations out of computational necessity, intermode-coupling is captured in a mean-field or perturbative treatment,[42] providing a further point of contrast between our work and previous DFT-based calculations.

Altogether, our simulations, along with the comments about anharmonicity and interaction models above, suggest that other phenomena are at play in stabilising I_h over I_c; in particular, our results predict that NQE play an important role too. To help understand why, Fig. 2(A) shows the different contributions to the free energy difference between I_h and I_c. Here, it is clear that the free energy change on moving from classical mechanics to a quantum-mechanical description of the nuclei predominantly accounts for stabilisation of I_h, resulting in a stabilisation of around 30 J/mol on top of the $\sim$10 J/mol found in our classical simulations. Furthermore, the different *intermolecular* and *intramolecular* contributions to the quantum-to-classical free-energy change can also be separated in our q-TIP4P/F simulations; these results, shown in Fig. 2(B), clearly demonstrate that the stabilisation upon including NQEs comes from the *intermolecular* interaction terms. In other words, NQEs induce changes in the I_h and I_c structures such that intermolecular interactions in I_h are preferentially stabilised relative to I_c.

Some initial insights into the role of NQEs in modifying the relative intermolecular interaction energies of I_h and I_c can be understood by considering the molecular geometries of the water molecules in classical and quantum mechanical simulations; details are shown in Fig.

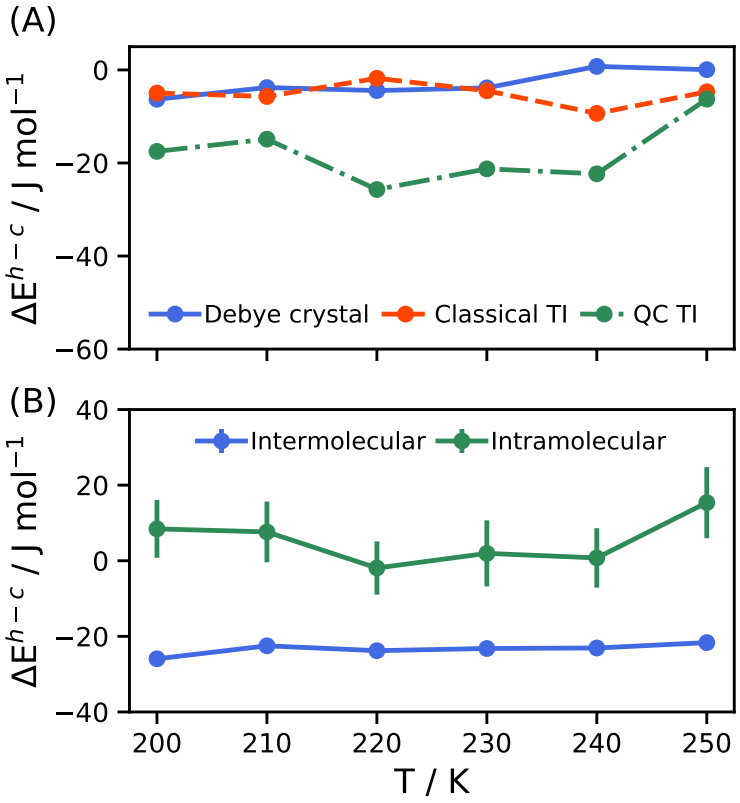

FIG. 2: (A) Major contributions to free energy differences between I_h and I_c; the Debye crystal contribution and classical TI term go into calculating the classical free energy; addition of the quantum-classical (QC) TI term leads to the calculated quantum free energy. (B) The QC TI difference contribution can be broken down into contributions from the intermolecular and intramolecular energy; the most important contribution is from changes the intermolecular term.

3. The classical molecular simulation results (Fig. 3, upper panels) show that there are small but definite differences in the geometry of water molecules in I_h and I_c. In the intramolecular part of the O-H RDF, the difference distribution (calculated in all cases as $f(I_h) - f(I_c)$) shows that there is a very slight shift to smaller O-H bond-lengths in I_h, although we find that the net effect on the average bond-lengths is similar in magnitude to the associated error bars in the calculation. In the case of the molecular H-O-H bond-angle distribution, the characteristic shape of the difference distribution for the classical simulation shows that the bond angle distribution for I_c shifts probability from lower to higher bond angles when compared to I_h.

Now consider the same results but from quantum simulations accounting for NQEs (lower panels, Fig. 3); the difference distributions are markedly different from those found in clas-

sical simulations. In particular, we find that differences in the O-H bond lengths, the H-O-H intramolecular bond angles and the molecular dipole moments are all effectively "washed out" by NQEs. This arises because of the well-known effect of NQEs on intermolecular hydrogen-bonding, which tends to be weakened by the inclusion of ZPE.[21,27,43] However, because the *classical* bond-angle distributions are different for I_h and I_c, this indicates that the change in the intramolecular energy on going from classical to quantum-mechanical simulations will also be different; this effect is observed in Fig. 2, where it is found that the change in the intramolecular free energy contribution for I_h is greater than that in I_c, as suggested by the differing behaviour of the bond angle distributions.

This effect carries through to the molecular dipole moment, which depends on both the O-H bond length and the H-O-H bond angle. The fact that the molecular dipole difference distribution is identical in shape and symmetry to the bond angle difference distribution indicates that changes in the bond angle are responsible for changes in the dipole distribution. Reflecting the angular distribution, the dipole distribution suggests a very slight shift to larger dipole moments in I_c relative to I_h. Given that the molecular dipole moment is a representative guide of intermolecular interaction strength in models such as q-TIP4P/F, these results that the flexibility of the q-TIP4P/F model allows a very slight strengthening of instantaneous intermolecular interactions in I_c compared to that observed in I_h. This intermolecular interaction strengthening effect again appears to be "washed out" when NQEs are included in the simulations, suggesting that the difference in free energy apparent in Fig. 2 is driven more through destabilization of I_c, rather than stabilization of I_h.

The impact on the intermolecular energies upon including NQEs can be more clearly visualized by mapping interactions between different dimers in the I_h and I_c structures, as in Fig. 4. Here, 5×10^6 water dimer configurations were extracted from either classical or quantum PIMD simulations. In the case of PIMD simulations, the atomic coordinates of a single ring-polymer bead were extracted; due to the cyclic invariance of the ring-polymer, the actual identity of the chosen bead does not matter. For each dimer, the intermolecular interaction energy was calculated; Figs. 4(A) and 4(B) show the quantum-classical difference between these distributions for I_h and I_c, respectively, plotted as a function of O-O distance and energy. We note that, because q-TIP4P/F uses an intermolecular pair potential, the interaction energy between a pair of dimers calculated in vacuum is the same as the interaction energy of the same dimer pair in the solid.

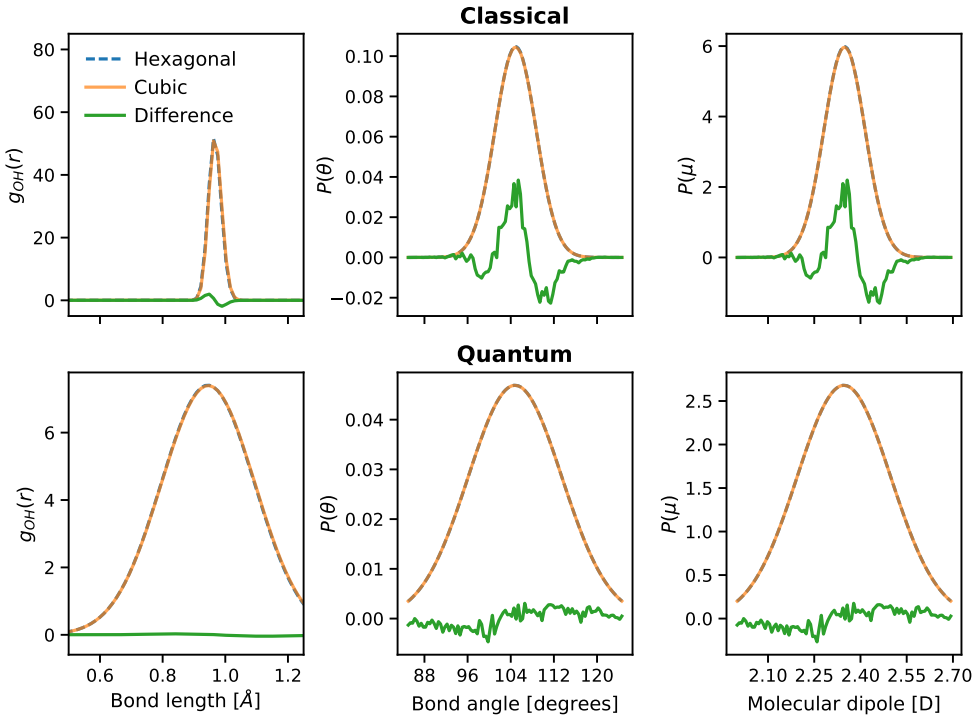

FIG. 3: Calculated O-H RDFs (left column), H-O-H bond-angle distributions (centre column) and molecular dipole momentum distribution (right column) determined in classical simulations (top row) and quantum (path-integral) simulations (bottom row). In each case, the distributions are shown for I_h and I_c. The difference between these two is also illustrated; in the case of the bond-angle and dipole distributions, the difference distribution is scaled by a factor of 100 for clarity.

In the case of I_c, these plots reveal that the changes in the intermolecular interactions upon quantization are quite small; the difference distribution appears to be reasonably featureless across the sampled range. However, in the case of I_h, there are clear features which suggest changes in the intermolecular interaction energy distribution within both the short-range and long-range dimer pairs. This complexity of interaction strengths is clearly evident in Fig. 4(A), where a strong pattern of changes in dimer interaction strengths is observed at distances of 5-6 Å. These distances correspond to second-nearest-neighbour water molecules and beyond. In seeking to rationalize where these changes come from, it is natural to consider the impact of NQEs on radial distribution functions (RDFs), as shown for H-H distances in Figs. 4(C) and (D). As has been pointed out by Needs *et al*, the I_h and I_c structures have different local hydrogen-bonding motifs as characterised by the presence of 'chair' and 'boat' conformations, which can give rise to distinct H-H RDFs for these structures beyond the

first coordination shell. This is evident in Fig. 4(C) where the *classical* RDFs have some differences in structure which can be attributed to the presence of distinct 'chair' and 'boat' forms (for example, Fig. 4(C) can be compared to Fig. 11 in reference 41); specifically, I_h comprises 'chair' and 'boat' hexagonal structures, whereas I_c comprises exclusively 'chair' structures. Upon inclusion of NQEs, these structural distinctions are largely washed away in both I_h and I_c; as a result, the dimer difference distributions of Fig. 4(A) and (B) are less related to whole-scale changes in structure, and are instead a consequence of small changes in hydrogen-bonding interactions which necessarily propagate through the crystal structure to preserve the ice rules. Our results thus lead us to speculate that the differing responses of 'chair' and 'boat' arrangements upon inclusion of NQEs gives rise to the observed difference in Fig. 4(A), and ultimately contribute significantly to the energy difference between I_h and I_c. Specifically, at least for the proton orderings which we have averaged over in our simulations, there is a suggestion that 'boat' hexamers may be preferentially stabilised in I_h; identifying exactly how this effect arises is a subject for future work.

To summarize, we have shown that (at least for the proton disordered configurations considered here) the empirical q-TIP4P/F water model predicts that NQEs stabilize I_h relative to I_c by around 30 J mol, and we have also sought to break down this stabilization effect into contributions from intramolecular geometry changes and intermolecular interactions. This has proven to be non-trivial, notably because of the fact that these two factors are interconnected, as noted in much previous work investigating 'competing quantum effects'.[21]

As a final point, during preparation of this manuscript we became aware of a study which has similarly investigated the influence of NQEs on the relative stability of I_c and I_h.[33] In this recent work, the authors combined DFT and sampling on machine-learned PESs to calculate the relative free energy of I_c and I_h. It is interesting to note that both our simulations (using an empirical force-field) and these other related simulations (using a DFT-based PES) reach similar conclusions regarding the important role of NQEs, while the observed trends in both empirical force-field simulations and DFT-based simulations give us some confidence in the reliability of q-TIP4P/F in these simulations. Together, these studies provide convincing evidence that subtle NQEs can lead to interesting phenomenon observed in macroscopic observables such as phase stability.

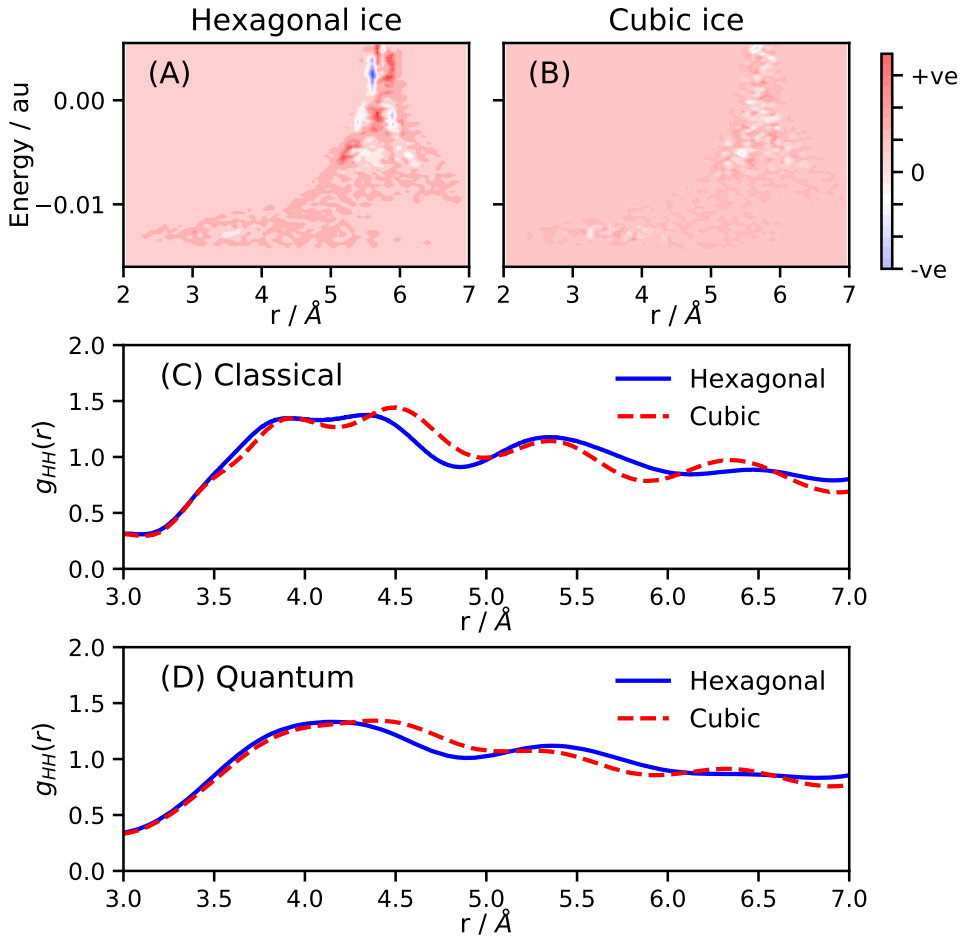

FIG. 4: (A) Quantum-Classical difference in dimer interaction energy distributions in I_h. (B) Quantum-Classical difference in dimer interaction energy distributions in I_c. (C) H-H radial distribution functions from classical simulations of I_h and I_c. (D) H-H radial distribution functions from quantum (PIMD) simulations of I_h and I_c.

IV. CONCLUSIONS

Overall, our simulation results suggest that NQEs play an important role in stabilising I_h relative to I_c, and contribute to the observation that bulk ice observed under typical atmospheric conditions is exclusively I_h. Our results suggest that changes to the intramolecular bond angle and dipole distributions upon quantization lead to destabilization of I_c; in addition, we have also shown how the related changes in hydrogen bonding lead to shifts in the relative energy of I_h and I_c such that $I_h$is stabilized. However, due to the complexity of

hydrogen-bonding patterns throughout the I_h and I_c structures, it is not straightforward to disentangle these two effects, or to decipher how changes to the hydrogen bonding network propagate through the structures; these investigations are left for ongoing work. Overall, our simulations add to the increasingly evidenced picture that NQEs play an important yet subtle in modifying molecular geometries and intermolecular interactions in liquids and solids.

SUPPLEMENTARY MATERIAL

Supplementary information, outlining the q-TIP4P/F interaction model, simulation details, free energy calculation methods and error estimates, is available online.

ACKNOWLEDGEMENTS

The authors gratefully acknowledge the Engineering and Physical Sciences Research Council (EPSRC) for the award of a studentship to SJB, and the Scientific Computing Research Technology Platform at the University of Warwick for providing computational resources.

DATA AVAILABILITY

Data from Figures 1, 2 and 3 can be found at http://wrap.warwick.ac.uk/110505.

REFERENCES

[1]K. Thurmer and S. Nie, Proc. Natl. Acad. Sci. USA **110**, 11757 (2013).

[2]Y. P. Handa, D. D. Klug, and E. Whalley, J. Chem. Phys. **84**, 7009 (1986).

[3]D. D. K. Y. P. Handa and E. Whalley, Can. J. Chem. **66**, 919 (1988).

[4]J. D. Bernal and R. H. Fowler, J. Chem. Phys. **1**, 515 (1933).

[5]T. L. Malkin, B. J. Murray, C. G. Salzmann, V. Molinero, S. J. Pickering, and T. F. Whale, Phys. Chem. Chem. Phys. **17**, 60 (2015).

[6]T. L. Malkin, B. J. Murray, A. V. Brukhno, J. Anwar, and C. G. Salzmann, Proc. Natl. Acad. Sci. USA **109**, 1041 (2012).

[7]D. Quigley, J. Chem. Phys. **141**, 121101 (2014).

[8]L. Lupi, A. Hudait, B. Peters, M. Grünwald, R. G. Mullen, A. H. Nguyen, and V. Molinero, Nature **551**, 218 (2017).

[9]E. A. Engel, B. Monserrat, and R. J. Needs, Phys. Rev. X **5**, 021033 (2015).

[10]H. Tanaka and I. Okabe, Chem. Phys. Lett. **259**, 593 (1996).

[11]E. Whalley, Can. J. Chem. **55**, 3429 (1977).

[12]C. Vega, C. Mcbride, E. Sanz, and J. L. F. Abascal, Phys. Chem. Chem. Phys. **7**, 1450 (2005).

[13]C. P. Herrero and R. Ramírez, J. Chem. Phys. **140**, 234502 (2014).

[14]H. Tanaka, J. Chem. Phys. **108**, 4887 (1998).

[15]J. L. F. Abascal and C. Vega, J. Chem. Phys. **123**, 234505 (2005).

[16]J. Abascal, E. Sanz, R. Fernandez, and C. Vega, J. Chem. Phys. **122** (2005).

[17]Z. Raza, D. Alfe, C. G. Salzmann, J. Klimes, A. Michaelides, and B. Slater, Phys. Chem. Chem. Phys. **13**, 19788 (2011).

[18]B. Pamuk, P. B. Allen, and M.-V. Fernández-Serra, Phys. Rev. B **92**, 134105 (2015).

[19]A. Hudait, S. Qiu, L. Lupi, and V. Molinero, Phys. Chem. Chem. Phys. **18**, 9544 (2016).

[20]T. Hondoh, T. Itoh, S. Amakai, K. Goto, and A. Higashi, J. Phys. Chem. **87**, 4040 (1983).

[21]S. Habershon, T. E. Markland, and D. E. Manolopoulos, J. Chem. Phys. **131**, 024501 (2009).

[22]S. Habershon, D. E. Manolopoulos, T. E. Markland, and T. F. Miller, Annu. Rev. Phys. Chem. **64**, 387 (2013).

[23]S. Habershon and D. E. Manolopoulos, J. Chem. Phys. **135**, 224111 (2011).

[24]S. Habershon and D. E. Manolopoulos, J. Chem. Phys. **131**, 244518 (2009).

[25]R. P. Feynman and A. R. Hibbs, *Quantum mechanics and path integrals* (McGraw-Hill, New York, 1965).

[26]M. Parrinello and A. Rahman, J. Chem. Phys. **80**, 860 (1984).

[27]A. Wallqvist and B. Berne, Chem. Phys. Lett. **117**, 214 (1985).

[28]S. Habershon and D. E. Manolopoulos, Phys. Chem. Chem. Phys. **13**, 19714 (2011).

[29]T. E. Markland and B. J. Berne, Proc. Nat. Acad. Sci. USA **109**, 7988 (2012).

[30]D. M. Wilkins, D. E. Manolopoulos, and L. X. Dang, J. Chem. Phys. **142**, 064509 (2015).

[31]V. Kapil, A. Cuzzocrea, and M. Ceriotti, J. Phys. Chem. B **122**, 6048 (2018).

[32]B. Pamuk, J. M. Soler, R. Ramírez, C. P. Herrero, P. W. Stephens, P. B. Allen, and M.-V. Fernández-Serra, Phys. Rev. Lett. **108**, 193003 (2012).

[33]B. Cheng, E. A. Engel, J. Behler, C. Dellago, and M. Ceriotti, Proc. Nat. Acad. Sci. USA **116**, 1110 (2019).

[34]S. W. Rick, J. Chem. Phys. **122**, 094504 (2005).

[35]S. Habershon, G. S. Fanourgakis, and D. E. Manolopoulos, J. Chem. Phys. **129**, 074501 (2008).

[36]X.-Z. Li, B. Walker, and A. Michaelides, Proc. Nat. Acad. Sci. USA **108**, 6369 (2011).

[37]M. J. Gillan, D. Alfé, and A. Michaelides, J. Chem. Phys. **144**, 130901 (2016).

[38]T. D. Kühne, M. Krack, and M. Parrinello, J. Chem. Theory Comput. **5**, 235 (2009).

[39]S. Yoo, X. C. Zeng, and S. S. Xantheas, J. Chem. Phys. **130**, 221102 (2009).

[40]J. C. Howard, J. D. Enyard, and G. S. Tschumper, J. Chem. Phys. **143**, 214103 (2015).

[41]J. M. Bowman, Y. Wang, H. Liu, and J. S. Mancini, J. Phys. Chem. Lett. **6**, 366 (2015).

[42]N. D. D. B. Monserrat and R. J. Needs, Phys. Rev. B **87**, 144302.

[43]R. A. Kuharski and P. J. Rossky, J. Chem. Phys. **82**, 5164 (1985).